Talanta 82 (2010) 348–358

Contents lists available at ScienceDirect

Talanta

journal homepage: www.elsevier.com/locate/talanta

Separation and quantification of $[RhCl_n(H_2O)_{6-n}]^{3-n}$ ($n = 0$–6) complexes, including stereoisomers, by means of ion-pair HPLC–ICP-MS

Wilhelmus J. Gerber[a,*], Klaus R. Koch[a], Hans E. Rohwer[b], Eric C. Hosten[b], Theodor E. Geswindt[a]

[a] Research Group of PGM Chemistry, Department of Chemistry and Polymer Science, Stellenbosch University, Private Bag XI, Stellenbosch 7602, Western Cape, South Africa
[b] Department of Chemistry, Nelson Mandela Metropolitan University, PO Box 77000, Port Elizabeth 6031, South Africa

ARTICLE INFO

Article history:
Received 6 January 2010
Received in revised form 22 April 2010
Accepted 23 April 2010
Available online 15 May 2010

Keywords:
Rh(III) aqua chlorido-complexes
Speciation
Ion-pair chromatography
Kinetics
HPLC
ICP-MS

ABSTRACT

A hyphenated ion-pair (tetrabutylammonium chloride—TBACl) reversed phase (C_{18}) HPLC–ICP-MS method (High Performance Liquid Chromatography Inductively Coupled Plasma Mass Spectroscopy) for anionic Rh(III) aqua chlorido-complexes present in an HCl matrix has been developed. Under optimum chromatographic conditions it was possible to separate and quantify cationic Rh(III) complexes (eluted as a single band), $[RhCl_3(H_2O)_3]$, *cis*-$[RhCl_4(H_2O)_2]^-$, *trans*-$[RhCl_4(H_2O)_2]^-$ and $[RhCl_n(H_2O)_{6-n}]^{3-n}$ ($n = 5$, 6) species. The $[RhCl_n(H_2O)_{6-n}]^{3-n}$ ($n = 5$, 6) complex anions eluted as a single band due to the relatively fast aquation of $[RhCl_6]^{3-}$ in a 0.1 mol L^{-1} TBACl ionic strength mobile phase matrix. Moreover, the calculated $t_{1/2}$ of 1.3 min for $[RhCl_6]^{3-}$ aquation at 0.1 mol kg^{-1} HCl ionic strength is significantly lower than the reported $t_{1/2}$ of 6.3 min at 4.0 mol kg^{-1} $HClO_4$ ionic strength. Ionic strength or the activity of water in this context is a key parameter that determines whether $[RhCl_n(H_2O)_{6-n}]^{3-n}$ ($n = 5$, 6) species can be chromatographically separated. In addition, aquation/anation rate constants were determined for $[RhCl_n(H_2O)_{6-n}]^{3-n}$ ($n = 3$–6) complexes at low ionic strength (0.1 mol kg^{-1} HCl) by means of spectrophotometry and independently with the developed ion-pair HPLC–ICP-MS technique for species assignment validation. The Rh(III) samples that was equilibrated in differing HCl concentrations for 2.8 years at 298 K was analyzed with the ion-pair HPLC method. This analysis yielded a partial Rh(III) aqua chlorido-complex species distribution diagram as a function of HCl concentration. For the first time the distribution of the *cis*- and *trans*-$[RhCl_4(H_2O)_2]^-$ stereoisomers have been obtained. Furthermore, it was found that relatively large amounts of 'highly' aquated $[RhCl_n(H_2O)_{6-n}]^{3-n}$ ($n = 0$–4) species persist in up to 2.8 mol L^{-1} HCl and in 1.0 mol L^{-1} HCl the abundance of the $[RhCl_5(H_2O)]^{2-}$ species is only 8–10% of the total, far from the 70–80% as previously proposed. A 95% abundance of the $[RhCl_6]^{3-}$ complex anion occurs only when the HCl concentration is above 6 mol L^{-1}. The detection limit for a Rh(III) species eluted from the column is below 0.147 mg L^{-1}.

1. Introduction

Separation and refining of platinum group metals (PGM) is based predominantly on the subtle difference between their anionic chlorido-complexes such as $[PtCl_6]^{2-}$, $[PdCl_4]^{2-}$, $[RhCl_6]^{3-}$ and $[IrCl_6]^{2/3-}$, while Ru and Os are generally separated by means of oxidative distillation [1,2]. Currently, rhodium is recovered last from PGM mining feed streams in South Africa using either solvent-extraction or ion-exchange followed by precipitation [2]. A possible reason for the 'late' recovery of Rh(III) is presumably due to the presence of aquated species, $[RhCl_n(H_2O)_{6-n}]^{3-n}$ ($n = 3$–5), even in strong chloride media [2,3]. To design more efficient refining methods, chemical speciation and the quantification of Rh(III) aqua chlorido-complexes in process solutions is of critical importance. The need for a detailed investigation of the species distribution of Rh(III) aqua chlorido-complexes in an HCl matrix is clearly reflected by the large differences between proposed species distribution diagrams, e.g. the reported HCl concentrations where a 1:1 ratio of $[RhCl_6]^{3-}$ and $[RhCl_5(H_2O)]^{2-}$ species exist varies from 0.04 to 8.3 mol L^{-1} HCl [3]. These large differences between proposed species distribution diagrams are indicative of the difficulty involved to develop an analytical technique for the separation and quantification of Rh(III) aqua chlorido-complexes present in an HCl matrix.

Sandström and co-workers [4,5] was able to characterize all $[RhX_n(H_2O)_{6-n}]^{3-n}$ ($X = Cl^-$, Br^- and $n = 0$–6) complexes, while Mann and Spencer [6] characterized the series of $[RhCl_nBr_{6-n}]^{3-n}$ ($n = 0$–6) complex anions by means of ^{103}Rh NMR. Unfortunately the relatively low magnetogyric ratio of the ^{103}Rh nucleus precludes ^{103}Rh NMR for relatively rapid speciation and quantification, particularly in dilute solutions [4–7]. Recent capillary electrophoresis (CE) speciation studies of Rh(III) present in several acidic

* Corresponding author. Tel.: +27 021 808 2699; fax: +27 021 808 3342.
E-mail address: wgerber@sun.ac.za (W.J. Gerber).

0039-9140/$ – see front matter © 2010 Elsevier B.V. All rights reserved.
doi:10.1016/j.talanta.2010.04.049

matrices (HCl, HNO_3, H_2SO_4) illustrated that several Rh(III) species could be separated with some peaks tentatively assigned to particular species [8–11]. However, separation and unambiguous assignment of in particular $[RhCl_n(H_2O)_{6-n}]^{3-n}$ (n = 2–4) stereoisomers has not yet been reported using any chromatographic technique. UV–VIS spectroscopy is of 'limited' use for speciation of Rh(III) aqua chlorido-complexes when more than two species are simultaneously present, due to the relatively small difference in molar extinction coefficient spectra of $[RhCl_n(H_2O)_{6-n}]^{3-n}$ (n = 0–6) species coupled with discrepancies between reported molar extinction coefficient spectra [12,13]. Matrix-assisted laser desorption ionization time-of-flight mass spectrometry (MALDI-TOF) does not reflect the species distribution in solution and cannot differentiate between stereoisomers, e.g. *cis*- or *trans*-$[RhCl_4(H_2O)_2]^-$ [11].

As part of our interest in developing speciation techniques for PGM [14–16] complexes present in HCl solutions similar to mining feed and effluent streams, we aimed to develop an ion-pair reversed phase (C_{18}) chromatographic speciation method for $[RhCl_n(H_2O)_{6-n}]^{3-n}$ (n = 0–6) species including stereoisomers, followed by detection by means of inductively coupled plasma mass spectrometry (ICP-MS). Despite the relatively 'uncomplicated' sample matrix (water and hydrochloric acid) the chromatographic separation and identification of these complexes is challenging due to the difference in the net charge, the kinetic lability of Rh(III) complexes and presence of stereoisomers which might be expected to exhibit only subtle retention differences in a chromatographic separation. Moreover, the mobile phase composition for a reversed phase ion-pair chromatographic separation is inevitably different from the HCl sample matrix which may lead to the interconversion of kinetically labile Rh(III) aqua chlorido-complexes [17–23] during a chromatographic run. This matter is exemplified by Salvadó and co-workers [11] who argued that the relatively rapid aquation of $[RhCl_6]^{3-}$ made it impossible to observe a peak for $[RhCl_6]^{3-}$ using CE, whereas Aleksenko et al. [10] claims the contrary. In this regard, we re-investigated the anation/aquation kinetics of Rh(III) aqua chlorido-complexes to evaluate the extent of species interconversion that might be expected during a chromatographic run. In particular, the rate of aquation at low ionic strength (0.1 mol L^{-1} HCl) conditions was studied since previous investigations [17–23] were conducted at relatively high ionic strengths ($\geq$2.0 mol L^{-1} HCl or $HClO_4$); such conditions are not compatible with the intended reversed phase ion-pair chromatographic separation. The assignment of eluted Rh(III) aqua chlorido-complexes by this means entailed a detailed kinetic study utilizing the developed reversed phase chromatographic speciation method and when possible results were compared for validation with an independent UV–VIS study conducted in parallel. This paper describes the development of an ion-pair HPLC–ICP-MS method for the separation and the quantification of $[RhCl_n(H_2O)_{6-n}]^{3-n}$ (n = 0–6) complexes present in an HCl matrix without the need for chelation of the metal cation [24] by ligands such as dithiocarbamates and 8-hydroxyquinoline prior to separation.

2. Experimental

2.1. Apparatus

The HPLC instrumentation used comprises of a Shimadzu LC-9A pump coupled to a Perkin-Elmer Sciex Elan 6100 ICP quadrupole MS detector (for breakthrough curve determination a Shimadzu CDD-6A conductivity detector was used) and steel tubing with inner diameter of 0.20 mm. The injection valve used was a Rheodyne (model number 7125) mounted with a 20 μL sample loop. The flow rate (u) of the mobile phase was 1.0 mL min^{-1}. The cylindrical steel columns had lengths (L) varying between 5 and 25 cm and an inner diameter (D_C) of 0.5 cm with mirror-finish interior walls. The room temperature was regulated at 25 ± 1 °C. The general ICP-MS operating conditions used were; nebulizer argon gas flow 0.97 L min^{-1}, ICP RF-Power 1100 W, isotope used: m/z 103, nebulizer type: cross flow. UV–VIS spectra were recorded with a Perkin-Elmer Lambda 12 double-beam UV–VIS spectrometer. Quartz cuvettes were used and the slit width was set at 1 nm. The room temperature was regulated at 25 ± 1 °C. A Grant KD100 circulating thermostatic controller, mounted on a Grant W6 tank with cooling coil, was used to regulate the temperature when the sample is prepared and within the sample chamber of the spectrometer at 25.0 ± 0.1 °C. pH measurements were performed using a Metrohm 691 pH-meter and a Metrohm 6.0232.100 combined glass pH electrode. Potentiometric standardization titrations were recorded and performed using a Metrohm 716 DMS Titrino with Metrohm 728 stirrer. A Metrohm 6.0404.100 combined massive silver electrode was used for argentiometric determination of chloride and bromide anions.

2.2. Reagents

0.1 mol L^{-1} stock solutions of tetrabutylammonium chloride (TBACl), tetrabutylammonium bromide (TBABr), potassium bromide (KBr) and tetrabutylphosphonium bromide (TBPBr) (Fluka) were prepared and used for subsequent dilutions. All solution preparations used Milli-Q water with resistivity levels of 18.1 MΩ cm. The stationary phase was Silica gel 100 C_{18} (Fluka 60757, CAS 112926-00-8). The C_{18} surface coverage is 17–18% or 4.0 μmol m^{-2} and the remaining surface hydroxyl groups are end-capped with methyl. The silica column material has an average diameter of 50 μm and the pore diameter is approximately 100 Å. Ethanol absolute, CH_3CH_2OH (Saarchem), was used as discussed in the column preparation section. Several stock Rh(III) solutions of approximately 1 mmol L^{-1} and 0.1 mol L^{-1} were prepared by dissolving $[RhCl_3]\cdot x(H_2O)$ (Alfa Aesar) in water at the desired HCl concentration. Total Rh concentration was determined using the ICP-MS and calibration was done with a certified multi-element PGM standard (Spectrascan 8313).

2.3. C_{18} column packing and conditioning

The "tap-fill" dry-pack method [25] was used for column packing. Evidence that the columns were properly packed was inferred from the 'perfect' Gaussian peak shape of eluted analytes, Fig. 1a, which implies no column voids and upon opening the columns no bed compression was found after weeks of use.

The reversed phase column was initially conditioned by passage of an ethanol/water (80:20, v/v) mixture through the column for at least 40 min, after which elution of the EtOH was affected by passage of a mobile phase that contained ion-pair reagent dissolved in water at the desired concentration for approximately 3 h [26]. After these conditioning steps the columns were ready for use. When a column was not used for an extended time period it was stored in 100% EtOH.

2.4. Chromatographic injection procedure for all Rh(III) samples

As an example, 1.0 mL of a ~1.0×10^{-3} mol L^{-1} Rh(III) stock sample was first diluted, 100-fold, to a total volume of 100.00 mL, such that the matrix of the diluted sample was 0.1 mol L^{-1} HCl at 298 K. The diluted sample was thoroughly mixed by means of a magnetic follower for ±45 s, after which a 20 μL aliquot of the diluted sample was injected onto the C_{18} column. The time taken from stock sample dilution until injection was, on average, approximately 114 s.

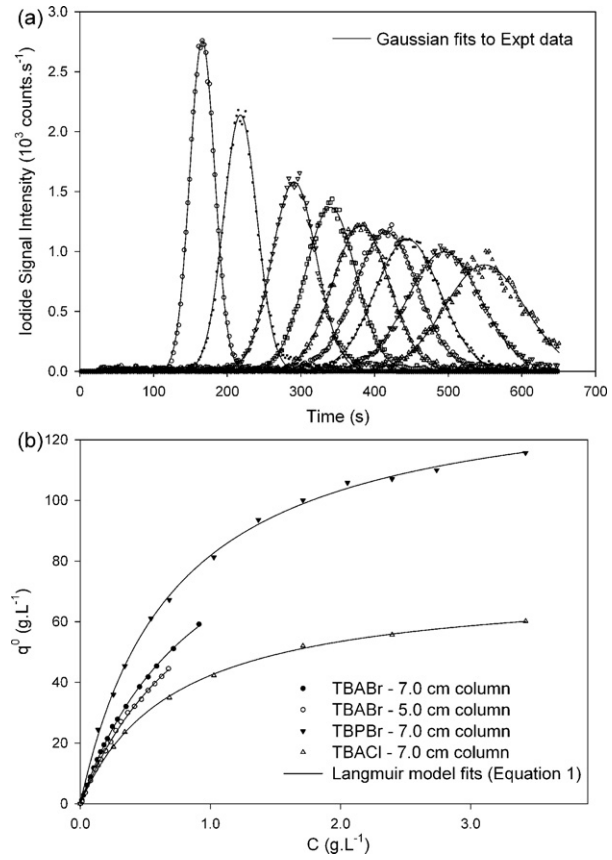

Fig. 1. (a) Typical iodide test sample Gaussian chromatographic traces as a function of mobile phase TBACl concentration. Column length = 5.0 cm, mobile phase = distilled water + (0.01, 0.015, 0.02, . . ., 0.05 M) TBACl + 0.01 mol L^{-1} HCl. (b) Ion-pair adsorption isotherms obtained by means of frontal analysis and the corresponding Langmuir model fits. The composition of the mobile phases consisted of the relevant ion-pair reagent dissolved in water.

2.5. Adsorption isotherm measurements by means of frontal analysis

One pump of the HPLC instrument was used to deliver a mobile phase that consists of water. A second pump delivered a mobile phase that consisted of ion-pair reagent (either TBABr or TBPBr or TBACl) dissolved in water. The break through curves shown in the supplemental information, Fig. S1a, were recorded successively at a flow rate of 1.0 mL min^{-1}, with an adequate delay between each break through curve to establish the re-equilibration of the column with the mobile phase that consists only of water. Using a set of KBr solutions of known concentration, the conductivity signal response was shown to be proportional to the injected KBr concentration. KBr is not retained at all in the column and effectively takes the column hold-up volume into account, Fig. S1b.

3. Computational details

3.1. The Langmuir isotherm

The Langmuir model [27] relates the amount of ion-pair reagent adsorbed, q^o, to the mobile phase concentration of ion-pair reagent, C, Eq. (1); where q_s is the monolayer saturation capacity and K_{ad} is the adsorption equilibrium constant:

$$q^o = q_s \left(\frac{K_{ad} C}{1 + K_{ad} C} \right) \quad (1)$$

The amount of ion-pair reagent adsorbed is given by Eq. (2), where V_{eq}, V_a and C are the elution volume, volume of the stationary phase and ion-pair mobile phase concentration, respectively:

$$q^o = \frac{C V_{eq}}{V_a} \quad (2)$$

3.2. Kinetic data analysis

The program Kinetic$_5$Ver [28] (Visual Basic 6) was written for the least-squares fitting of rate law(s), derived from reaction models, to experimental data (spectrophotometric and chromatographic). The program has two main components that work in tandem; a routine to numerically integrate the differential equations using a Runge–Kutta algorithm [29] and a routine to execute the least-squares fitting using the Simplex algorithm [30]. Validation of program, Kinetic$_5$Ver, was performed by generating artificial data via analytical integration of several rate models in varying complexity with chosen rate constants and molar extinction coefficients. The artificial data sets were then manipulated with the aid of a random number generator such that each data point had an absolute error varying from 0 to 3%. These augmented data sets were then analyzed with program Kinetic$_5$Ver and in all cases the calculated parameters with Kinetic$_5$Ver agreed within 2% with the chosen parameters used in the analytical integration.

3.3. Mauser plots

The theory of Mauser space diagrams has been extensively discussed by Polster and co-worker [31,32]. In particular, we were interested in the absorbance triangle plot for a linear reaction system (e.g. relation (3)) with two consecutive reactions in order to calculate the molar extinction coefficients from UV–VIS spectra for several Rh(III) species:

$$A \rightarrow B \rightarrow C \quad (3)$$

To obtain all the molar extinction coefficients in the wavelength region (390–550 nm) would require literally, 25,600 absorbance (λ_y) versus absorbance (λ_x) plots. This large amount of graphs results from plotting all wavelengths against each other. To achieve this task, a program called Mauser$_1$Ver was written in VB.Net [33].

4. Results and discussion

4.1. Ion-pair C_{18} HPLC column capacity and column overload

The extent of separation or resolution between Rh(III) aqua chlorido-complexes can be controlled by varying the surface concentration of ion-pair reagent, column length and competing ion-pair reactions. The surface concentration of ion-pair reagent (TBACl, TBABr, TBPBr) at a specific mobile phase ion-pair reagent concentration and the column monolayer saturation capacity, q_s, were determined by means of frontal analysis. The adsorption isotherms obtained and the least-squares fits with the Langmuir model, Eq. (1), are shown in Fig. 1b. The good least-squares fits, Fig. 1b, combined with the agreement in the calculated column monolayer saturation capacity, Table 1, using different ion-pair reagents and column lengths validate the Langmuir model. The calculated adsorption constants, K_{ad}, are listed in Table 1.

Relatively rapid interconversion of Rh(III) aqua chlorido-complexes (due to aquation or anation) during a chromatographic run as well as column overload [34], will result in non-Gaussian peak shapes. To estimate at what ion-pair reagent concentration column overload occurred in this ion-pair HPLC system, sodium iodide test samples were injected as a function of mobile phase ion-pair concentration, Fig. 1a. The sample matrix of the iodide test

Table 1
From the Langmuir model fits the C_{18} monolayer saturation capacity, q_s, and ion-pair reagent adsorption constants, K_{ad}, at 298 K were calculated. The internal diameter of these columns was 0.2 cm. L = column length.

Ion-pair reagent	K_{ad} (L g^{-1})	q_s (g L^{-1})	L (cm)
TBABr	1.03 (±0.04)	120 (±5)	7.0
TBABr	0.99 (±0.06)	132 (±4)	5.0
TBPBr	1.43 (±0.04)	137 (±8)	7.0
TBACl	0.78 (±0.05)	128 (±8)	7.0

samples were the same as for the injected Rh(III) samples and the highest concentration of iodide was 20 times that of the total Rh(III) concentration injected in this study. As 'perfect' iodide Gaussian peaks (Fig. 1a) were obtained, column overload can be ruled out as a possible cause for non-Gaussian peak shapes obtained in this study (*vide infra*). Moreover, to monitor column degradation and to measure the efficiency of newly packed columns, daily injection of the iodide test samples were carried out.

4.2. Kinetic based speciation of $[RhCl_n(H_2O)_{6-n}]^{3-n}$ (n = 3–6) at low HCl ionic strength

The difficulty of assigning Rh(III) aqua chlorido-complexes that elute during a chromatographic separation is due, in part, that several Rh(III) species are simultaneously present even at relatively high HCl concentrations [2]. This problem was addressed by exploiting the well documented *trans* effect [17–23,35] when Rh(III) aqua chlorido-complexes undergo ligand exchange reactions. Of particular interest in this study was the possible stereo-specific substitution of successive aquation of the $[RhCl_6]^{3-}$ complex anion based on the *trans* effect, i.e. $[RhCl_6]^{3-} \rightarrow [RhCl_5(H_2O)]^{2-} \rightarrow$ *cis*-$[RhCl_4(H_2O)_2]^{-} \rightarrow$ *fac*-$[RhCl_3(H_2O)_3]$ [12]. This reaction sequence was exploited for Rh(III) species assignment since it is relatively easy to carry out practically, by diluting a Rh(III) sample equilibrated in concentrated HCl (>9.0 mol L^{-1}) to a 0.1 mol L^{-1} HCl matrix and following this process by UV–VIS spectroscopy. Harris and co-workers [12,17–19] conducted extensive kinetic studies concerning the ligand exchange rates of Rh(III) aqua chlorido-complexes. However, the ionic strength at which these investigations were conducted varied from approximately 2 mol kg^{-1} (HCl or $HClO_4$) upwards and are not suitable (*vide infra*) for an ion-pair reversed phase chromatographic separation. As the ionic strength can significantly alter the rate of ligand exchange, we re-investigated the aquation rates of $[RhCl_n(H_2O)_{6-n}]^{3-n}$ (n = 4–6) species in a relatively low ionic strength environment of 0.1 mol kg^{-1} HCl. A 0.1 mol L^{-1} ionic strength was chosen since it closely resembles the mobile phase composition used in this study and the kinetic study is likely to establish the extent by which Rh(III) species interconversion might occur during a chromatographic run. In addition, comparison of the kinetic data (*vide infra*) obtained with the UV–VIS study and independently with the developed ion-pair HPLC–ICP-MS study, enable the correct assignment of the Rh(III) aqua chlorido-complexes separated chromatographically.

Available species distribution diagrams suggest that in a 9.5 mol L^{-1} HCl matrix only $[RhCl_6]^{3-}$ and $[RhCl_5(H_2O)]^{2-}$ species are present in significant quantities [3]. Dilution of a stock Rh(III) sample equilibrated in 9.464 mol L^{-1} HCl to a 0.101 mol L^{-1} HCl matrix results in relatively rapid successive aquation reactions of the Rh(III) species. The ensuing UV–VIS spectral change was monitored as a function of time at 298.1 K, Fig. 2a. The first set of isosbestic points formed within 6 min, indicated by the solid vertical lines in Fig. 2a, after which a second set of isosbestic points was observed as indicated by the vertical dashed lines. The two sets of isosbestic points confirm that only two Rh(III) species are predominant at a time during the sequential aquation reactions (4) and (5),

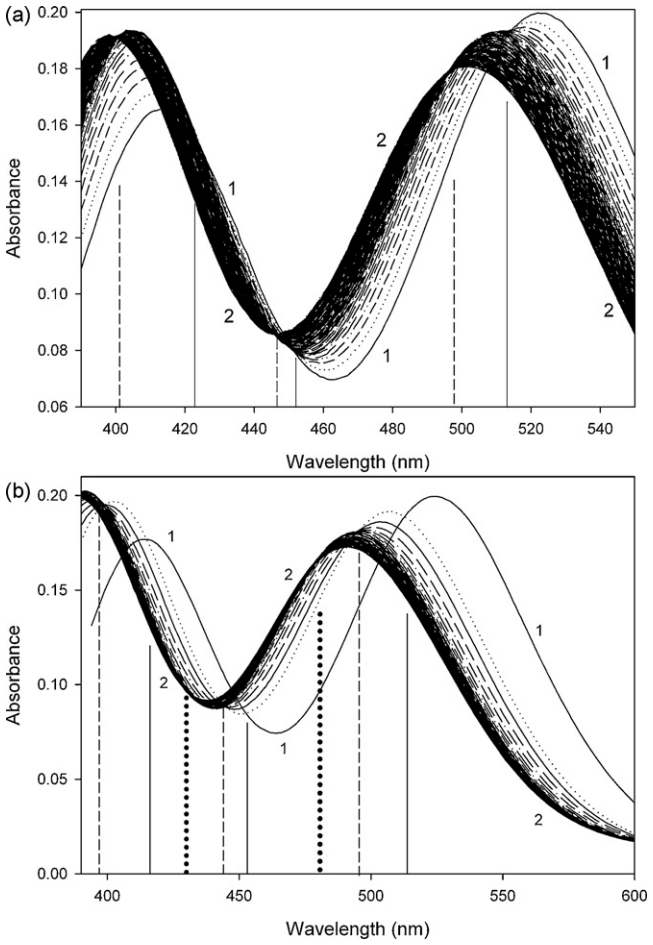

Fig. 2. The UV–VIS spectral change as a function of time when diluting a 0.1963 mol L^{-1} Rh(III) sample equilibrated in 9.464 mol L^{-1} HCl, 100-fold, to a 0.101 mol L^{-1} HCl matrix, (a) represents the first 90 min and (b) 3 days of recording after dilution. Solid, dashed and dotted vertical lines indicate the three sets of isosbestic points observed and are associated with the successive aquation reactions $[RhCl_6]^{3-} \rightarrow [RhCl_5(H_2O)]^{2-} \rightarrow$ *cis*-$[RhCl_4(H_2O)_2]^{-} \rightarrow$ *fac*-$[RhCl_3(H_2O)_3]$, respectively.

respectively. Moreover, the second set of isosbestic points corroborate that aquation of $[RhCl_5(H_2O)]^{2-}$ is most likely to yield only the *cis*-$[RhCl_4(H_2O)_2]^{-}$ stereoisomer, as a result of the higher *trans* effect of the coordinated chloride ion compared to water [17].

From Fig. 2a it is observed that 90 min after dilution the rate by which the UV–VIS spectrum change decrease considerably. This is associated with the relatively slower rate of aquation of the *cis*-$[RhCl_4(H_2O)_2]^{-}$ complex and it was therefore necessary to record the UV–VIS spectrum of the diluted sample over a period of at least 4 days to observe the formation of the third set of isosbestic points at 431 and 478 nm, Fig. 2b. The third set of isosbestic points confirm the stereo-specific substitution route of successive aquation reactions, leading to the conclusion that aquation of *cis*-$[RhCl_4(H_2O)_2]^{-}$ yields the *fac*-$[RhCl_3(H_2O)_3]$ stereoisomer, relation (6):

$$[RhCl_6]^{3-} + H_2O \underset{k_{56}}{\rightleftharpoons} [RhCl_5(H_2O)]^{2-} + Cl^- \quad (4)$$

$$[RhCl_5(H_2O)]^{2-} + H_2O \underset{k_{45}}{\overset{k_{54}}{\rightleftharpoons}} cis\text{-}[RhCl_4(H_2O)_2]^{-} + Cl^- \quad (5)$$

$$cis\text{-}[RhCl_4(H_2O)_2]^{-}_{(aq)} + H_2O \underset{k_{34}}{\overset{k_{43}}{\rightleftharpoons}} fac\text{-}[RhCl_3(H_2O)_3] + Cl^- \quad (6)$$

For the calculation of the relevant aquation/anation rate constants from the data, of which Fig. 2a is a typical example, the same rate laws, Eqs. (7)–(9), proposed by Harris and co-workers

Table 2
Comparison of the calculated Rh(III) aqua chlorido-complexes pseudo-first-order aquation and anation rate constants by means of UV–VIS spectroscopy and independently with the ion-pair HPLC method at 298.1 K and 0.101 mol kg^{-1} HCl ionic strength.

Aquation/anation rate constants	Experimental technique		
	UV–VIS	Ion-pair HPLC–ICP-MS	Literature[a]
k_{65} (min^{-1})	$5.52\ (\pm0.23)\times10^{-1}$	–	1.1×10^{-1}[b]
k_{54} (min^{-1})	$1.51\ (\pm0.07)\times10^{-2}$	$1.48\ (\pm0.06)\times10^{-2}$[c]	2.32×10^{-3}[b]
cis–fac k_{43} (min^{-1})	$1.24\ (\pm0.04)\times10^{-4}$	$1.31\ (\pm0.05)\times10^{-4}$[d] $1.28\ (\pm0.06)\times10^{-4}$[e] $1.26\ (\pm0.07)\times10^{-4}$[f]	–
fac–cis k_{34} (M^{-1} min^{-1})	$3.46\ (\pm0.11)\times10^{-4}$	$3.52\ (\pm0.14)\times10^{-4}$[d] $3.49\ (\pm0.17)\times10^{-4}$[f]	–
trans–mer k_{43} (min^{-1})	–	$4.28\ (\pm0.21)\times10^{-4}$[e] $4.32\ (\pm0.23)\times10^{-4}$[f]	–
mer–trans k_{34} (M^{-1} min^{-1})	–	$1.42\ (\pm0.03)\times10^{-4}$[f]	–

The corresponding pseudo-first-order anation rate constants calculated were negligibly small at 0.1 mol kg^{-1} HCl ionic strength experimental conditions.
[a] Refs. [3,17].
[b] Aquation rate constants determined at 4.0 mol kg^{-1} ionic strength.
[c] Fig. 4c.
[d] Fig. 5c.
[e] Fig. 8c.
[f] Fig. 8d.

[12,17] three decades ago were used. Due to the significant lower rate of aquation of *cis*-$[RhCl_4(H_2O)_2]^-$ compared to $[RhCl_5(H_2O)]^{2-}$, the aquation of *cis*-$[RhCl_4(H_2O)_2]^-$ was not included in the reaction model fitted. Using the program Kinetic$_5$Ver the rate laws, Eqs. (7)–(9), were simulated and non-linear least-squares regression fits at several wavelengths were carried out. The agreement between the experimental and simulated data is excellent and the fit at 550 nm is shown in Fig. 3a. The good least-squares fits validate the rate laws and the calculated rate constants listed in Table 2 are the average of at least four separate experiments:

$$\frac{d(A)}{dt} = -k_{65}(A) + k_{56}(B)(Cl^-) \quad (7)$$

$$\frac{d(B)}{dt} = k_{65}(A) - k_{56}(B)(Cl^-) - k_{54}(B) + k_{45}(E)(Cl^-) \quad (8)$$

$$\frac{d(E)}{dt} = k_{54}(B) - k_{45}(E)(Cl^-) \quad (9)$$

$A = [RhCl_6]^{3-}$, $B = [RhCl_5(H_2O)]^{2-}$ and E = *cis*-$[RhCl_4(H_2O)_2]^-$.

We find that the pseudo-first-order aquation rate constants, k_{65} and k_{54}, are much larger compared with those reported in literature [3,17], Table 2. As ionic strength is the only difference between our experiments and that reported in the literature [17], the effect of ionic strength on the rate of aquation was investigated at a fixed chloride concentration of 0.1 mol L^{-1}. This was done by diluting a Rh(III) sample equilibrated in 9.464 mol L^{-1} HCl such that the matrix of the diluted sample contained 0.101 mol L^{-1} HCl and the desired concentration of $HClO_4$, which was varied from 0.1 to 5.6 mol L^{-1}. From Fig. 3a it is observed that as the ionic strength increase, the rate of aquation associated with reactions (4) and (5) decreases substantially. The least-squares fits obtained using program Kinetic$_5$Ver are shown in Fig. 3a and the computed rate constants are listed in Table 3. The calculated aquation rate constants, k_{65} and k_{54}, Table 3 at an ionic strength of 4.0 mol kg^{-1} $HClO_4$ agree satisfactorily with those reported by Harris and co-worker [17] (Table 2) and validates our kinetic analyses. The relatively large decrease of the aquation rates with an increase in ionic strength can be attributed to a decrease of the activity of water and the Rh(III) aqua chlorido-complexes.

In order to calculate the relevant aquation/anation rate constants for reaction (6) from the data, of which Fig. 2b is a typical example, the rate laws, Eqs. (7), (8) and (10), were used. Similar as before, using the program Kinetic$_5$Ver Eqs. (7), (8) and (10) were

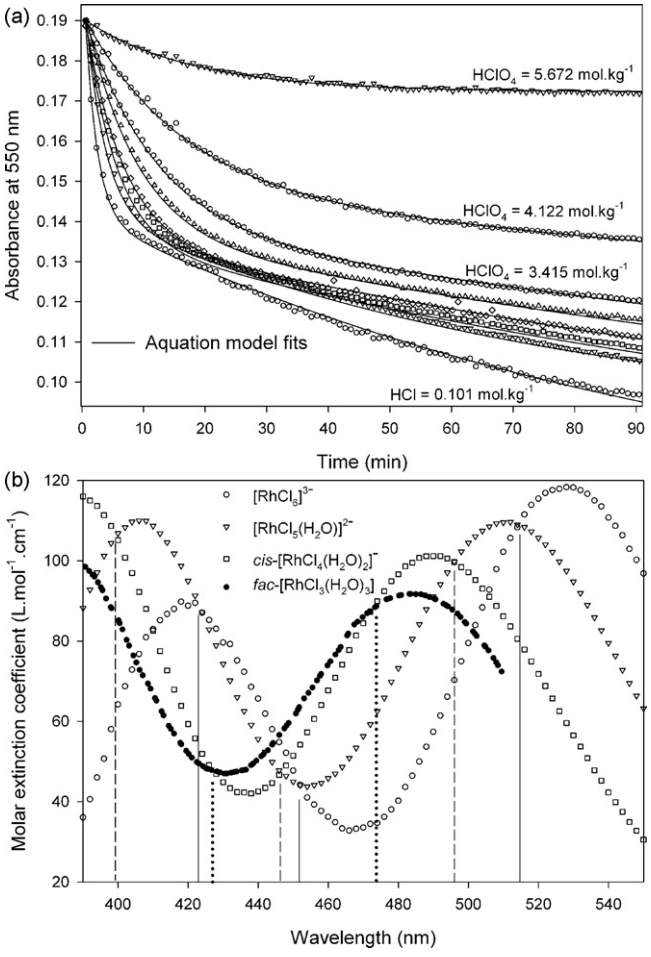

Fig. 3. (a) The symbols represent the absorbance change as a function of time when diluting 0.1963 mol L^{-1} Rh(III) samples equilibrated in 9.464 mol L^{-1} HCl, 100-fold, to a 0.101 mol L^{-1} HCl and specified concentration of $HClO_4$. The aquation model least-squares fits (solid lines) are excellent and the concentrations of $HClO_4$ used in each case are listed in Table 3. (b) Calculated molar extinction coefficients for $[RhCl_n(H_2O)_{6-n}]^{3-n}$ (n = 3–5) complexes using the program Mauser$_1$Ver.

Table 3
Calculated pseudo-first-order aquation rate constants for the $[RhCl_n(H_2O)_{6-n}]^{3-n}$ (n = 5, 6) complex anions as a function of ionic strength (perchloric acid) at 298.1 K.

Ionic strength	Aquation rate constants	
$HClO_4$ (mol kg^{-1})	k_{65} (min^{-1})	k_{54} (min^{-1})
0.109	$5.42\ (\pm0.21)\times10^{-1}$	$1.53\ (\pm0.05)\times10^{-2}$
0.912	$3.15\ (\pm0.17)\times10^{-1}$	$1.26\ (\pm0.04)\times10^{-2}$
1.84	$2.03\ (\pm0.13)\times10^{-1}$	$6.77\ (\pm0.33)\times10^{-3}$
2.34	$1.62\ (\pm0.08)\times10^{-1}$	$4.94\ (\pm0.19)\times10^{-3}$
2.66	$1.21\ (\pm0.08)\times10^{-1}$	$4.01\ (\pm0.16)\times10^{-3}$
3.41	$8.78\ (\pm0.29)\times10^{-2}$	$2.40\ (\pm0.07)\times10^{-3}$
4.12	$6.19\ (\pm0.31)\times10^{-2}$	$1.64\ (\pm0.05)\times10^{-3}$
5.66	$4.66\ (\pm0.23)\times10^{-2}$	–

simulated and non-linear least-squares regression fits at several wavelengths resulted in excellent agreement between the experimental and simulated data illustrated for 490 and 520 nm in the supplementary information, Fig. S2. The calculated aquation and anation rate constants, k_{43} and k_{34}, are listed in Table 2:

$$\frac{d(E)}{dt} = k_{54}(B) - k_{43}(E) + k_{34}(G)(Cl^-) - k_{45}(E)(Cl^-) \quad (10)$$

$B = [RhCl_5(H_2O)]^{2-}$, $E = cis$-$[RhCl_4(H_2O)_2]^-$ and $G = fac$-$[RhCl_3(H_2O)_3]$.

The least-squares fits to the kinetic data discussed above not only yield the relevant aquation/anation rate constants but also the molar extinction coefficients of the Rh(III) aqua chlorido-complexes at several wavelengths. To further validate the kinetic analyses, the molar extinction coefficients of $[RhCl_5(H_2O)]^{2-}$, cis-$[RhCl_4(H_2O)_2]^-$ and fac-$[RhCl_3(H_2O)_3]$, were independently re-calculated using Mauser diagrams, Fig. 3b. A typical Mauser diagram obtained with program Mauser$_1$Ver is shown in the supplementary data, Fig. S3. The agreement between the molar extinction coefficients calculated for the Rh(III) complexes with the two differing computational methods is excellent and confirm the results from the kinetic analyses performed. The molar extinction coefficient spectrum for $[RhCl_6]^{3-}$ could not be calculated from the Mauser plots and it was assumed as in the literature [12,13], that in concentrated (>9 mol L^{-1}) HCl essentially only the $[RhCl_6]^{3-}$ species is present. The calculated molar extinction coefficient spectra for the $[RhCl_n(H_2O)_{6-n}]^{3-n}$ (n = 3–5) species intersect at all the experimentally found isosbestic points and indicates that the aquation/anation model used is internally consistent, Fig. 3b. Interestingly, the UV–VIS molar extinction coefficients for the $[RhCl_n(H_2O)_{6-n}]^{3-n}$ (n = 3–6) species reported by Kleinberg and co-workers [13] and Harris and co-worker [12] differ substantially from one another, but our calculated ε data agree well with those reported by Harris and co-worker [12].

4.3. Chromatographic separation and the assignment of $[RhCl_6]^{3-}$, $[RhCl_5(H_2O)]^{2-}$, cis-$[RhCl_4(H_2O)_2]^-$ and fac-$[RhCl_3(H_2O)_3]$ complexes

The need for a speciation analysis of Rh(III) aqua chlorido-complexes in an HCl matrix is clearly reflected by the large differences between proposed species distribution diagrams [3]. In order to measure the concentration of a Rh(III) species when several $[RhCl_n(H_2O)_{6-n}]^{3-n}$ (n = 0–6) aqua chlorido-complexes are simultaneously present with the proposed ion-pair HPLC–ICP-MS speciation method, it is first necessary to assign the separated Rh(III) species. Utilizing the kinetic results obtained from the UV–VIS study above, which confirmed a stereo-specific substitution course of successive aquation of the $[RhCl_6]^{3-}$ complex anion, assignment of several of the Rh(III) aqua chlorido-complexes of interest separated with the ion-pair HPLC method (*vide infra*) becomes possible. A crucial component of the separation 'step' is that the Rh(III) aqua chlorido-complexes speciation must not change. This is potentially problematic for the separation of $[RhCl_5(H_2O)]^{2-}$ and $[RhCl_6]^{3-}$ species since the $t_{1/2}$ for aquation of the $[RhCl_6]^{3-}$ species was found to be 1.3 min at 0.1 mol kg^{-1} HCl ionic strength and 298 K in contrast to 4.5 min [17] at 4.0 mol kg^{-1} HCl ionic strength. Hence to minimize aquation of the $[RhCl_6]^{3-}$ complex anion during a chromatographic run, the intended separation should be completed as rapidly as possible and at 'high' ionic strength. It was found that a 5.0 cm column and a mobile phase of 0.1 mol L^{-1} TBACl, 0.01 mol L^{-1} HCl and water gave the best results in terms of a relatively rapid ion-pair HPLC separation. Diluting a Rh(III) sample equilibrated in 9.464 mol L^{-1} HCl to a 0.101 mol L^{-1} HCl matrix, followed by injection of the diluted sample as a function of time yields the chromatographic traces shown in Fig. 4a and b. From the UV–VIS data it can be confidently inferred that 10 min after dilution the sample only contains the $[RhCl_5(H_2O)]^{2-}$ and cis-$[RhCl_4(H_2O)_2]^-$ complex anions to any significant extent. It is thus reasonable that the Rh(III) species which elutes at 90 s (Fig. 4b), 10 min after dilution can be assigned to the $[RhCl_5(H_2O)]^{2-}$ species. Quantification of the Rh(III) species was done by integrating the entire transient signal and individual peaks. Division of individual peak area by the total transient signal area yields the mole fraction of a Rh(III) species. Multiplication of the mole fraction of a species with the known total Rh concentration yields the individual Rh(III) species concentration. A plot of $\ln([RhCl_5(H_2O)]^{2-})$ versus time, Eq. (11), yields a linear trend (Fig. 4c) confirming a pseudo-first-order aquation reaction. The aquation rate constant, k_{54}, obtained from the slope of the linear regression fit in Fig. 4c agree quantitatively with the k_{54} calculated for the $[RhCl_5(H_2O)]^{2-}$ species from the UV–VIS data (Table 2) confirming the assignment here. Moreover, when the diluted sample was injected 5.4 h after preparation, which is sufficient time for all the $[RhCl_5(H_2O)]^{2-}$ species to undergo aquation to form the cis-$[RhCl_4(H_2O)_2]^-$ species, no Rh(III) eluted at 90 s and proves that $[RhCl_n(H_2O)_{6-n}]^{3-n}$ (n = 0–4) species do not elute at 90 s. It is now apparent that the relatively broad peak in Fig. 4a at 90 s is due to a combination of $[RhCl_5(H_2O)]^{2-}$ and $[RhCl_6]^{3-}$ species. The relatively fast aquation of $[RhCl_6]^{3-}$ and the fact that a dilution step before injection is necessary makes it difficult or nearly impossible to choose chromatographic conditions with this system such that peaks for both $[RhCl_6]^{3-}$ and $[RhCl_5(H_2O)]^{2-}$ species can be observed in agreement with the CE study done by Salvadó and co-workers [11]:

$$\ln([B]_o) = -k_{54}t + \ln([B]_i) \quad (11)$$

The chromatographic conditions used to separate cis-$[RhCl_4(H_2O)_2]^-$ and $[RhCl_5(H_2O)]^{2-}$, Fig. 4b, is clearly not appropriate for the separation of $[RhCl_n(H_2O)_{6-n}]^{3-n}$ (n = 3, 4) complexes including stereoisomers. The optimum chromatographic parameters found for such a separation of $[RhCl_n(H_2O)_{6-n}]^{3-n}$ (n = 3, 4) complexes was determined to be a column of length 25.0 cm and the mobile phase consisted of water, 0.05 mol L^{-1} TBACl and 0.01 mol L^{-1} HCl. Diluting a stock Rh(III) sample equilibrated in 9.464 mol L^{-1} HCl to a 0.101 mol L^{-1} HCl matrix, followed by injection of the diluted sample as a function of time yielded the chromatographic traces shown in Fig. 5a and b. The pronounced tailing observed beyond 600 s in Fig. 5a for the sample injected 2.5 min after dilution suggests that only $[RhCl_5(H_2O)]^{2-}$ and $[RhCl_6]^{3-}$ complex anions are present shortly after dilution and considerable aquation of these species occurs during the chromatographic run. The second injection of the diluted Rh(III) sample (Fig. 5a) was 61 min after dilution and exhibit much less tailing compared to the first injection. The decrease in tailing is expected since 61 min after sample dilution all of the $[RhCl_6]^{3-}$ and approximately 66% of the $[RhCl_5(H_2O)]^{2-}$ species had undergone aquation to yield the cis-$[RhCl_4(H_2O)_2]^-$ species and therefore contains much less $[RhCl_5(H_2O)]^{2-}$ species that can

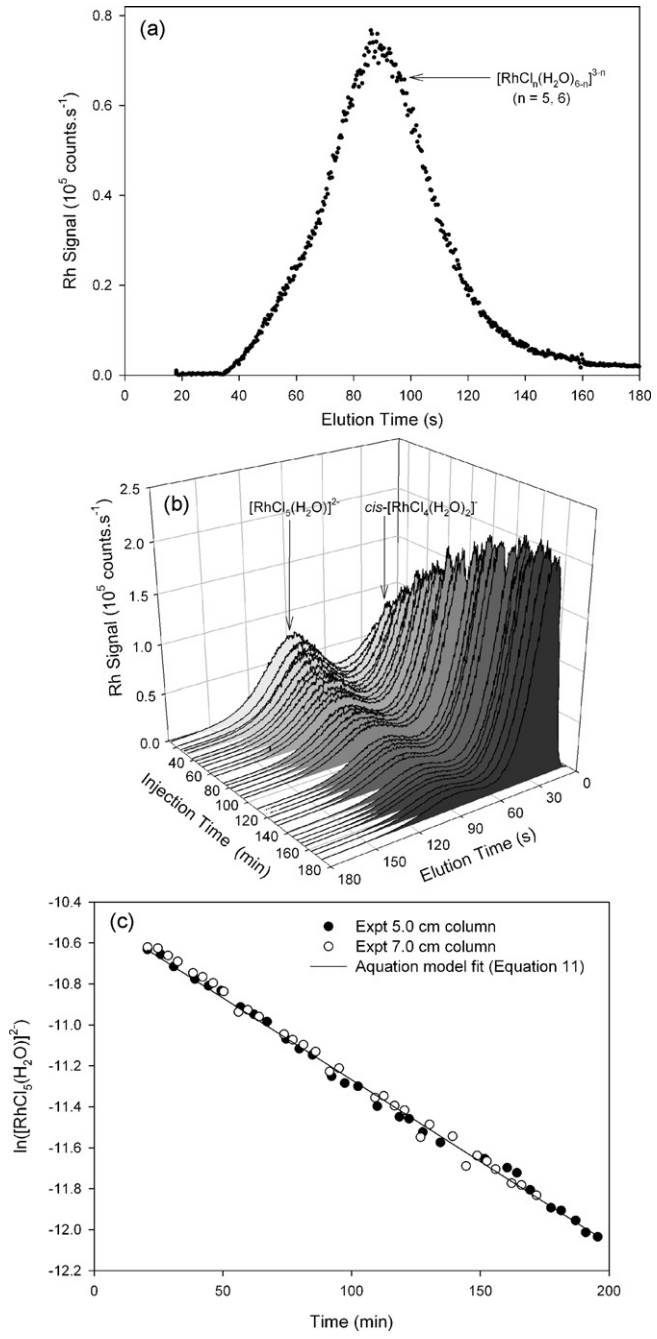

Fig. 4. Chromatographic traces obtained when diluting a 2.983 mmol L^{-1} Rh(III) sample equilibrated in 9.464 mol L^{-1} HCl, 100-fold, to a 0.101 mol L^{-1} HCl matrix and (a) injecting the sample immediately after dilution (114 s) and (b) as a function of time. (c) A plot of $\ln([RhCl_5(H_2O)]^{2-})$ versus time yielded a linear trend confirming pseudo-first-order aquation kinetics. Mobile phase = water + 0.1 mol L^{-1} TBACl + 0.01 mol L^{-1} HCl, column length = 5.0 cm. The RSD (relative standard deviation) for peak area determination was below 5%.

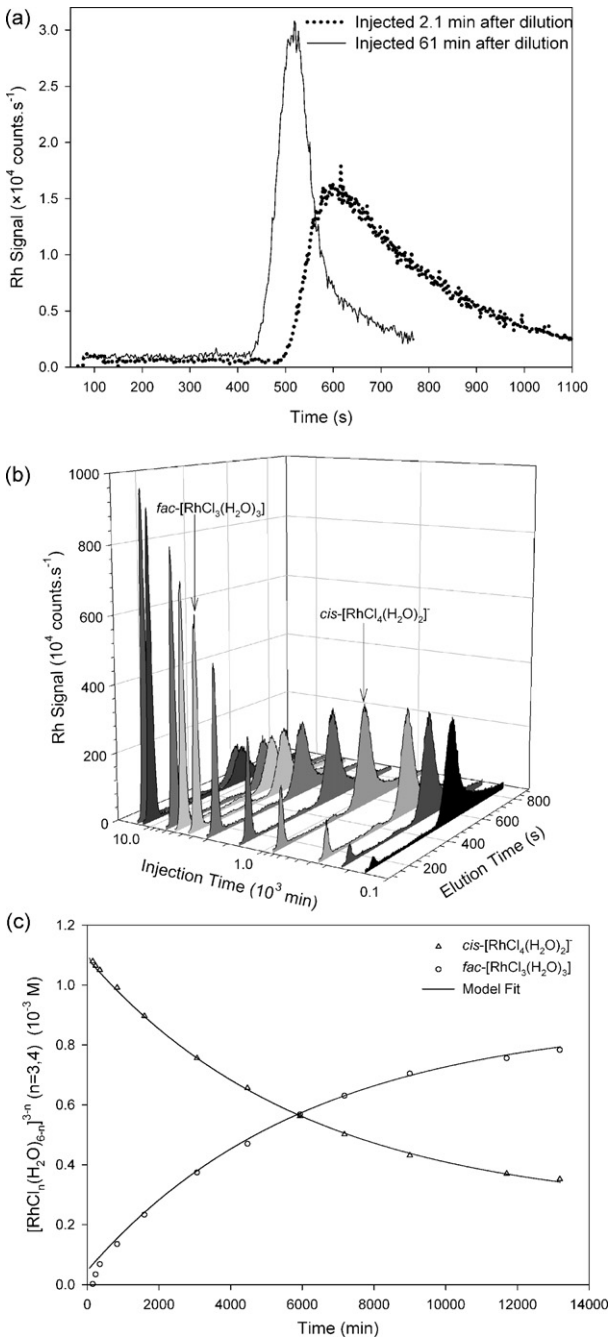

Fig. 5. Chromatographic traces (a) and (b) obtained when diluting a 0.1123 mol L^{-1} Rh(III) sample equilibrated in 9.464 mol L^{-1} HCl, 100-fold, to a 0.101 mol L^{-1} HCl matrix after which the diluted sample was injected as a function of time; (c) excellent aquation/anation model fit. Column length = 25.0 cm, mobile phase = water + 0.05 mol L^{-1} TBACl + 0.01 mol L^{-1} HCl.

aquate during the chromatographic run. In Fig. 5b the peak at 550 s initially intensify due to further aquation of $[RhCl_5(H_2O)]^{2-}$ and subsequently decreased in intensity with time. At the same time a peak at 180 s appears and only intensifies with time. These trends are consistent with the stereo-specific substitution course of successive aquation of the $[RhCl_6]^{3-}$ complex anion and it is thus reasonable to conclude that the peaks at 180 and 550 s are due to the *fac*-$[RhCl_3(H_2O)_3]$ and *cis*-$[RhCl_4(H_2O)_2]^-$ species, respectively. Simulation of the rate laws Eqs. (7), (8) and (10) using program Kinetic$_5$Ver resulted in an excellent least-squares fit to the data in Fig. 5b shown in Fig. 5c. The quantitative agreement between the calculated k_{43} and k_{34} rate constants, relation (6), determined chromatographically and independently with UV–VIS (Section 4.2 and Table 2) confirms the peak assignments.

In summary, the stereo-specific substitution course of successive aquation of the $[RhCl_6]^{3-}$ complex anion relations (4)–(6), were monitored using UV–VIS spectroscopy and independently with the ion-pair HPLC–ICP-MS method. The agreement between the UV–VIS and ion-pair HPLC data is excellent, Fig. 6, and the rate of each successive aquation reaction decreases by approximately an order of magnitude.

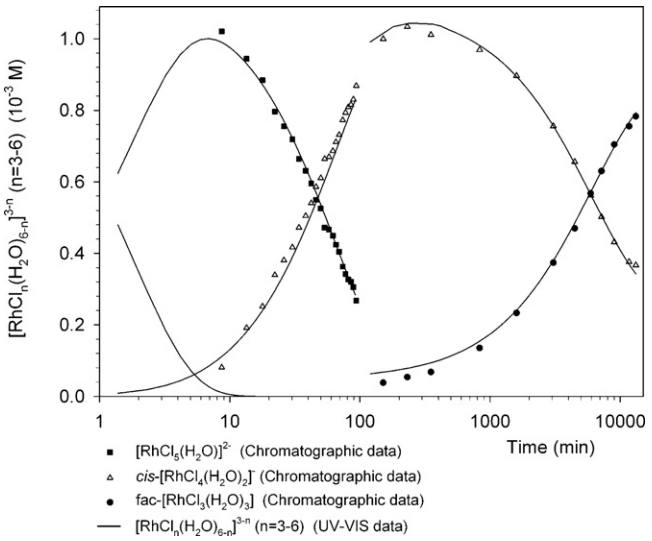

Fig. 6. Diluting a Rh(III) sample equilibrated in 9.462 mol L^{-1} HCl to a 0.101 mol L^{-1} HCl matrix results in successive aquation reactions. The calculated species concentration profiles from the UV–VIS data agree quantitatively with that determined 'directly' with the developed ion-pair HPLC speciation method and illustrate the internal consistency of the chromatographic peak assignments made.

4.4. 'Equilibrium' species distribution of $[RhCl_n(H_2O)_{6-n}]^{3-n}$ ($n = 0–6$) complexes as a function of HCl concentration

For the reaction conditions chosen in Sections 4.2 and 4.3, several of the Rh(III) aqua chlorido-complexes (cationic, *mer*-$[RhCl_3(H_2O)_3]$ and *trans*-$[RhCl_4(H_2O)_2]^-$) are not present in these solutions due to the stereo-specific substitution course of successive ligand exchange and the relatively slow aquation of the *cis*-$[RhCl_4(H_2O)_2]^-$ and *fac*-$[RhCl_3(H_2O)_3]$ species. Hence several stock Rh(III) samples were prepared with differing HCl concentration matrices (0.1–9.5 mol L^{-1} HCl) and allowed to equilibrate for ±2.8 years at 298 K. Injection of these Rh(III) stock samples resulted in the chromatographic traces shown in Fig. 7a and b. Before injection of a Rh(III) stock sample it is necessary to rapidly dilute it to a 0.1 mol L^{-1} HCl matrix, the time taken from dilution to injection was approximately 114 s for each sample.

For increasing HCl concentration in the stock samples, the area of the peak at 90 s (Fig. 7a) associated with the $[RhCl_n(H_2O)_{6-n}]^{3-n}$ ($n = 5$, 6) complex anions is seen to increase and for the stock sample with a 9.5 mol L^{-1} HCl matrix no peak is observed at 30 s. Despite the difficulty to obtain a clean baseline chromatographic separation of the $[RhCl_6]^{3-}$ and $[RhCl_5(H_2O)]^{2-}$ species, the chromatographic traces illustrated in Figs. 4a and 7a however represents an accurate technique to quantify the combined concentration of these complex anions present in a sample. During the dilution step and chromatographic run only approximately 5% of the $[RhCl_5(H_2O)]^{2-}$ species undergo aquation which slightly changes the species abundance relative to the undiluted sample, based on the rate of aquation data in Table 2.

The chromatographic traces shown in Fig. 7b exhibit several interesting features: (i) an un-retained peak at 120 s which decreases relatively fast in intensity as the chloride concentration in the Rh(III) stock solutions increase and above 4.0 mol L^{-1} chloride it was no longer observed. Although the manufacturer states that "all" residual surface silanol groups are endcapped with methyl, a relatively small percentage remain which can potentially act as cation-exchange sites. To obtain confirmation that cationic species is not retained several chloride salts Li^+, Na^+, Cs^+ and Ba^{2+} were injected separately under the same chromatographic conditions and concentration as done for the Rh(III) samples. All of the

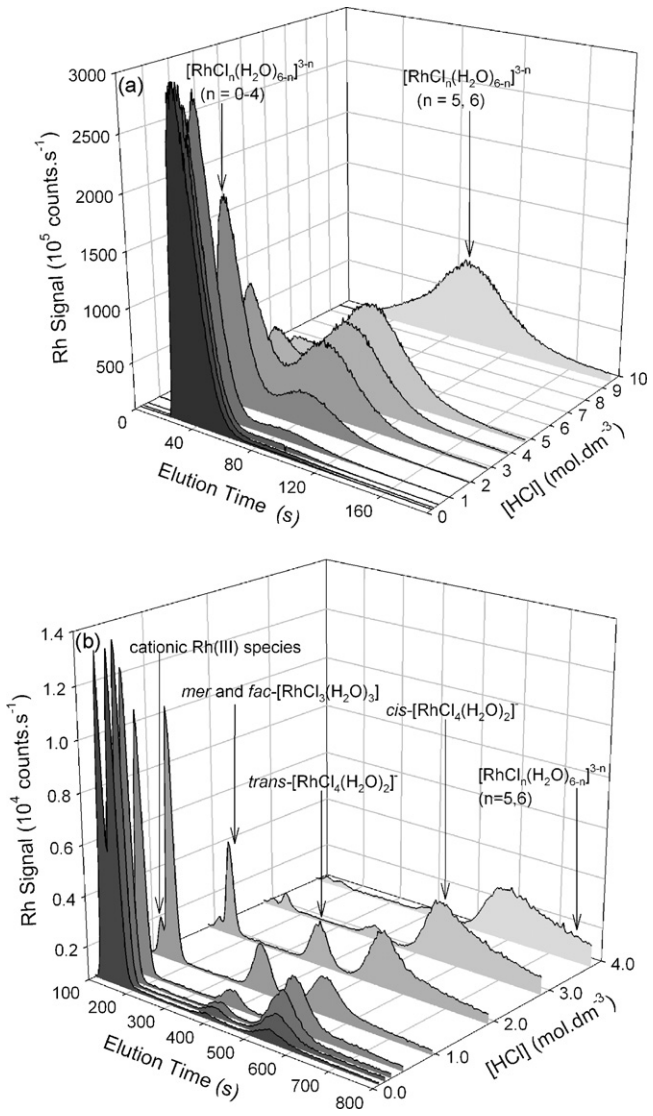

Fig. 7. Chromatographic traces (a) and (b) obtained when injecting the Rh(III) stock samples that were equilibrated in differing HCl matrices immediately (114 s) after dilution to a 0.101 mol L^{-1} HCl matrix. Total Rh(III) concentration for each sample was 1.283 mmol L^{-1}. Chromatographic conditions for (a) column length = 5.0 cm, mobile phase = water + 0.1 mol L^{-1} TBACl + 0.01 mol L^{-1} HCl and (b) column length = 25.0 cm, mobile phase = water + 0.05 mol L^{-1} TBACl + 0.01 mol L^{-1} HCl. The RSD for peak area determination in (a) and (b) was below 5 and 4%, respectively.

cationic metal ions eluted as Gaussian profiles at 120 s. Moreover, the TBA^+ concentration in the mobile phase is in 5000 times excess compared to the total Rh(III) concentration or the group 1 and 2 cationic metal ions injected and will strongly compete for the possible cation-exchange sites. As cationic species are not retained under the above-mentioned chromatographic conditions the peak at 120 s is assigned to cationic Rh(III) aqua chlorido-complexes. (ii) It was established that the Rh(III) species eluting at 180 s is due to the *fac*-$[RhCl_3(H_2O)_3]$ complex, Fig. 5b. During the 2.8 years that the Rh(III) stock solutions were aged it is accepted that the *mer*-$[RhCl_3(H_2O)_3]$ species will be present in addition to *fac*-$[RhCl_3(H_2O)_3]$. These Rh(III) complexes are not charged and it is possible that they are retained due to adsorption on the neutral C_{18} stationary phase. Another possible retention mechanism could be ascribed to partial hydrolysis of these species at the mobile phase pH of 2 to form $[RhCl_3(H_2O)_2(OH)]^-$ complex anions that can "ion-pair" with TBA^+. However, the reported pK_a values by

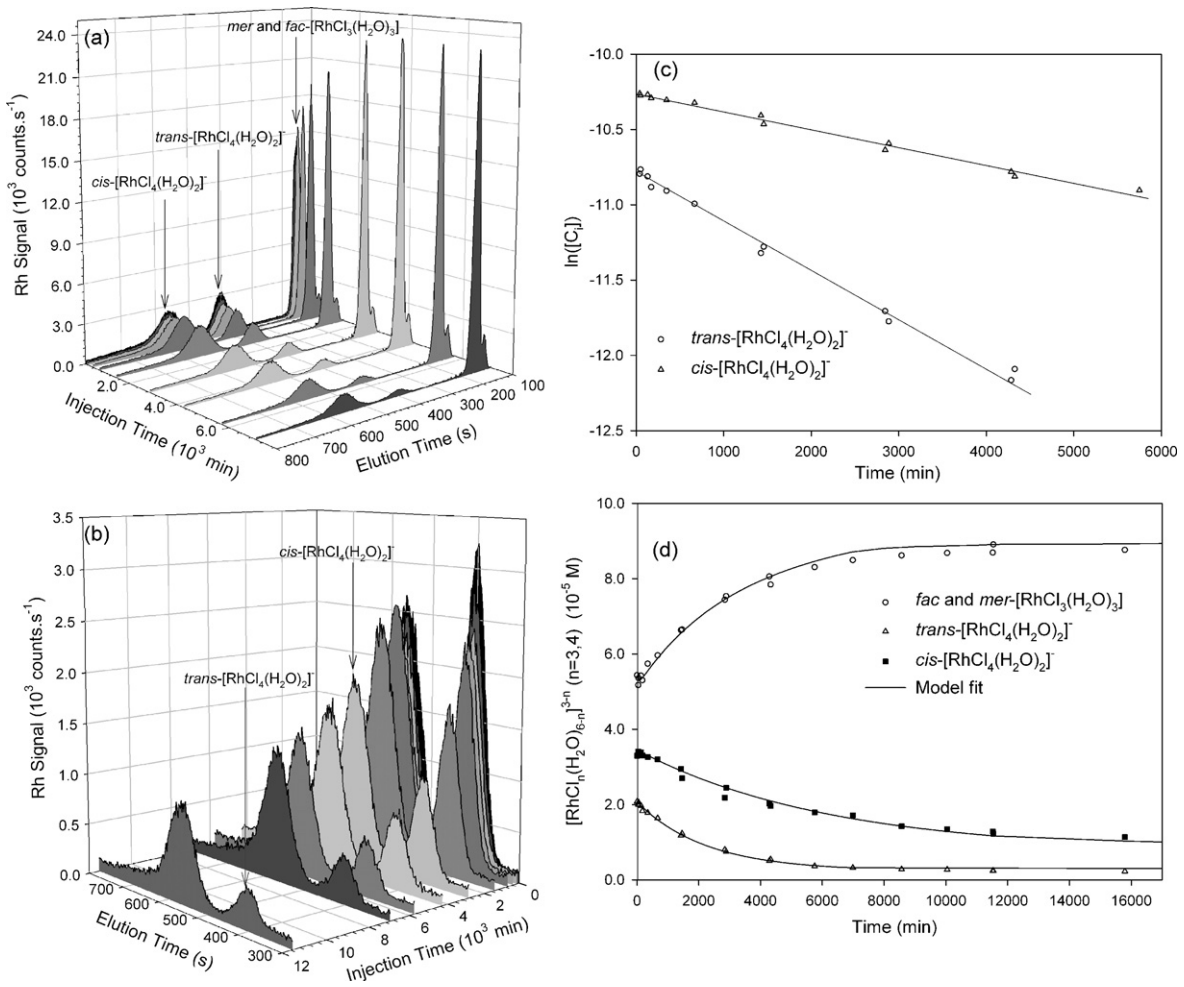

Fig. 8. Chromatographic traces obtained (a) when diluting a Rh(III) sample equilibrated in 9.464 mol L^{-1} HCl to a 0.998 mol L^{-1} HCl matrix and injecting the diluted sample as a function of time, (b) is an enlargement of the *cis*- and *trans*-$[RhCl_4(H_2O)_2]^-$ species elution profiles, (c) pseudo-first-order aquation model fits and (d) model fits that take into account anation in addition to aquation for the relevant species. Column length = 25.0 cm, mobile phase = distilled water + 0.05 mol L^{-1} TBACl + 0.01 mol L^{-1} HCl. The RSD for peak area determination is below 4%.

Harris and co-worker [12] of 7.31 and 6.96 for the *fac* and *mer* species respectively suggest that only a negligibly small fraction of these species are hydrolyzed at a pH of 2. Moreover, increasing the pH of the mobile phase to 7 (by replacing the added 0.01 mol L^{-1} HCl with 0.01 mol L^{-1} NaCl in the mobile phase) did not influence the retention times of eluting species. The intensity of the peak at 180 s decreases slower as the chloride concentration in the Rh(III) stock solutions increase compared to the peak at 120 s. This can be rationalized when considering that the *fac*- and *mer*-$[RhCl_3(H_2O)_3]$ species will increase relative to cationic Rh(III) species at higher chloride concentrations. For now, we tentatively assign the peak at 180 s to be a combination of *fac*- and *mer*-$[RhCl_3(H_2O)_3]$ and confirm this assumption below. (iii) It was conclusively shown that the *cis*-$[RhCl_4(H_2O)_2]^-$ species elutes at 550 s, Fig. 5b. To assign the peak at 400 s, Fig. 7b, the following should be noted; it is unlikely that the *mer*-$[RhCl_3(H_2O)_3]$ complex would exhibit such a large difference in retention behavior compared to the *fac*-$[RhCl_3(H_2O)_3]$ species, $[RhCl_n(H_2O)_{6-n}]^{3-n}$ ($n = 5$, 6) species undergo aquation during the chromatographic run which is the cause of the tailing beyond 600 s, the pK_a of *cis*-$[RhCl_4(H_2O)_2]^-$ species is larger than 7 ensuring negligible hydrolysis at a pH of 2 and the concentration of Rh(III) in the stock samples (~1.0 mmol L^{-1}) is to low for dimerization to occur. The only plausible species that remains is the *trans*-$[RhCl_4(H_2O)_2]^-$ complex anion and the peak at 400 s, Fig. 7b, is assigned as such. The *trans*-$[RhCl_4(H_2O)_2]^-$ species is present at highest concentration in a 1.0 mol L^{-1} HCl matrix taking several months to form when Rh(III) equilibrated in a 9.464 mol L^{-1} HCl is diluted to a 1.0 mol L^{-1} HCl matrix at 298 K. The relatively long time required for the formation of the *trans*-$[RhCl_4(H_2O)_2]^-$ species can be explained by the stereo-specific course of ligand substitution due to the *trans* effect, as proposed by Harris and co-worker [12], i.e. $[RhCl_6]^{3-} \rightarrow [RhCl_5(H_2O)]^{2-} \rightarrow$ *cis*-$[RhCl_4(H_2O)_2]^- \rightarrow$ *fac*-$[RhCl_3(H_2O)_3] \rightarrow$ *cis*-$[RhCl_2(H_2O)_4]^+ \rightarrow$ *mer*-$[RhCl_3(H_2O)_3] \rightarrow$ *trans*-$[RhCl_4(H_2O)_2]^-$.

According to the study by Harris and co-worker [12] the *trans*-$[RhCl_4(H_2O)_2]^-$ species undergoes aquation more rapidly than the *cis*-$[RhCl_4(H_2O)_2]^-$. In order to confirm the *mer*-$[RhCl_3(H_2O)_3]$ and *trans*-$[RhCl_4(H_2O)_2]^-$ peak assignments we measured the rate of aquation of the *cis*- and *trans*-$[RhCl_4(H_2O)_2]^-$ species. For these kinetic experiments, the Rh(III) stock solution equilibrated in a 0.995 mol L^{-1} HCl matrix for 2.8 years was diluted to a 0.101 mol L^{-1} HCl matrix, followed by injection of the diluted sample as a function of time. The results for one of these experiments are shown in Fig. 8a and b, from which it is observed that the peak at 550 s (*cis*-$[RhCl_4(H_2O)_2]^-$) initially increase due to the aquation of $[RhCl_5(H_2O)]^{2-}$ (first 150 min) after which the peaks at 400 and 550 s both decrease in intensity with time due to aquation of the *trans*- and *cis*-$[RhCl_4(H_2O)_2]^-$ species, respectively. The *cis*- and *trans*-$[RhCl_4(H_2O)_2]^-$ aquation products are the *fac*- and *mer*-$[RhCl_3(H_2O)_3]$ species respectively and it is observed (Fig. 8a) that only the peak at 180 s increase in intensity as a function of time, consistent with the assignment that the *fac*- and *mer*-

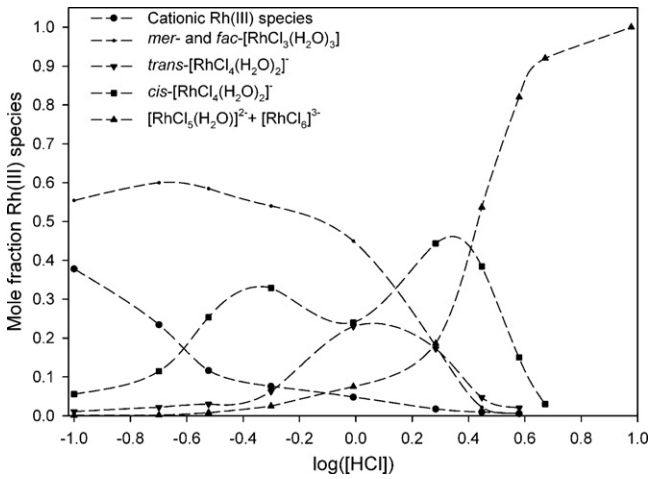

Fig. 9. $[RhCl_n(H_2O)_{6-n}]^{3-n}$ species distribution diagram as a function of HCl concentration. The total Rh(III) concentration for each sample was 1.283 mmol L^{-1}. The RSD for species abundance is below 5%.

$[RhCl_3(H_2O)_3]$ species elute as a single band at 180 s. Moreover, up to approximately 5000 min after dilution anation of *mer*- and *fac*-$[RhCl_3(H_2O)_3]$ is negligible and therefore plots of ln([*cis*- or *trans*-$[RhCl_4(H_2O)_2]^-$]) versus time, Eq. (11), were done and is illustrated in Fig. 8c. The good linear least-squares regression fits, Fig. 8c, confirmed pseudo-first-order aquation reactions and the calculated *cis* and *trans* k_{43} aquation rate constants are listed in Table 2. After 5450 min, anation of *mer*- and *fac*-$[RhCl_3(H_2O)_3]$ species must be taken into account and it was therefore necessary to do a non-linear least-squares fit with the rate model given by Eqs. (8), (10) and (12), as shown in Fig. 8d. The aquation rate constants calculated with the linear and non-linear least-squares fits, Table 2, agree quantitatively. Furthermore, the aquation rate constant for the *cis*-$[RhCl_4(H_2O)_2]^-$ complex agrees quantitatively with that determined previously using UV–VIS, Fig. S2, and chromatographically, Fig. 5, shown in Table 2. In addition, due to the *trans*-$[RhCl_4(H_2O)_2]^-$ species having two sites for chloride exchange compared to the one chloride site for the *cis*-$[RhCl_4(H_2O)_2]^-$ species, aquation of the *trans* stereoisomer is slightly faster than the *cis* stereoisomer.

$$\frac{d(F)}{dt} = -k_{43}(F) + k_{34}(H)(Cl^-) \quad (12)$$

F = *trans*-$[RhCl_4(H_2O)_2]^-$ and H = *mer*-$[RhCl_3(H_2O)_3]$.

A partial Rh(III) species distribution diagram as a function of HCl concentration, Fig. 9, was constructed by integrating the respective peaks in Fig. 7a and b. Due to the relatively fast aquation of $[RhCl_6]^{3-}$ only the combined amount of $[RhCl_n(H_2O)_{6-n}]^{3-n}$ (n = 5, 6) can be determined. Moreover, aquation of the $[RhCl_n(H_2O)_{6-n}]^{3-n}$ (n = 0–5) species is slow enough such that the speciation of the Rh(III) system do not change in the time taken to dilute and inject the stock samples. In addition, the chloride concentration in the diluted sample and in the mobile phase is always lower or equal to the Rh(III) stock samples and anation of Rh(III) species is therefore of no concern and will not change the species amounts during the dilution step or chromatographic run. Comparing our proposed speciation diagram with those shown in the review by Benguerel et al. [3] several differences are observed. Firstly, highly aquated $[RhCl_n(H_2O)_{6-n}]^{3-n}$ (n = 0–4) complexes persist in appreciable amounts up to 3.0 mol L^{-1} HCl. From a solvent- or solid phase extraction perspective [2,3] the most important difference occurs at 1.0 mol L^{-1} HCl where it was found that the $[RhCl_5(H_2O)]^{2-}$ species is only in 8–10% abundance which is in stark contrast to the data of Cozzi and Pantani [37] and Benguerel et al. [3] that claim 70 and 80% abundance, respectively. This large discrepancy was easily resolved with the following kinetic experiments. When Rh(III) equilibrated in 9.464 mol L^{-1} HCl was diluted to a 1.0 mol L^{-1} HCl matrix the UV–VIS spectral change as a function of time, Fig. S4a, clearly indicate that $[RhCl_5(H_2O)]^{2-}$ undergo significant aquation. From the kinetic model fit it is calculated, Fig. S4b, that only 44% of $[RhCl_5(H_2O)]^{2-}$ species remains after 90 min and it can be seen from Fig. S4b that significant aquation will continue to occur with time. Confirmation of these results were obtained by diluting Rh(III) equilibrated in 9.464 mol L^{-1} HCl to HCl matrices which varied from 0.1 to 6.5 mol L^{-1}, Fig. S5. The kinetic analyses performed on the data set shown in Fig. S5 clearly indicate that even in a 2.8 mol L^{-1} HCl matrix significant aquation of $[RhCl_5(H_2O)]^{2-}$ occurs. Interestingly only above a HCl concentration of 6 mol L^{-1}, no UV–VIS spectral change is observed as a function of time. This suggests that the $[RhCl_6]^{3-}$ species is in 95% or higher abundance when present in 6.0 mol L^{-1} HCl. These experiments confirm our chromatographic speciation data, Fig. 9, and also explains several anomalous Rh(III) extraction results found by Schmuckler and co-worker [1,36]. Moreover, the kinetic-based speciation diagram proposed by Benguerel et al. [3] only take into account $[RhCl_n(H_2O)_{6-n}]^{3-n}$ (n = 4–6) species thereby neglecting further aquation and stereoisomers. It should also be noted that our proposed species distribution diagram is as a function of HCl concentration and no attempt was made to keep ionic strength constant as done in literature [3,17,37], to better reflect actual industrial process solution conditions. Metal ions such as copper and strontium are not present in the samples prepared in this study and hence possible polyatomic interferences caused by $^{40}Ar^{63}Cu^+$ and $^{86}Sr^{16}OH^+$ are absent. The Rh(III) samples prepared in this study reflect what can be expected in the mining industry, since "all" base and platinum group metals are 'removed' prior to Rh recovery [2]. Moreover, the HPLC separation step can minimize polyatomic interference since each possible interfering species will presumably have a different retention time compared to the Rh(III) species and hence minimize possible peak overlap. In addition, metal ions present in group 1 and 2, such as ^{86}Sr in particular, will not form negatively charged chlorido complexes and will elute as an un-retained peak with no peak overlap with $[RhCl_n(H_2O)_{6-n}]^{3-n}$ (n = 3–6) species.

In addition to the Rh(III) species reported in several CE [9–11] studies, it was possible with the ion-pair HPLC technique to obtain a baseline separation of the $[RhCl_4(H_2O)_2]^-$ stereoisomers and assign them as well. In effect, more information regarding the speciation of Rh(III) aqua chlorido-complexes present in an HCl matrix, Fig. 9, was gained using the ion-pair HPLC technique compared to CE studies. Lastly, the ion-pair HPLC method has considerable scope for improvement by decreasing the column material particle size from 50 μm currently used to 5 μm or smaller and of course selecting different types of ion-pair reagents.

5. Conclusions

We developed an ion-pair (TBACl) reversed phase (C_{18}) HPLC–ICP-MS speciation method for Rh(III) aqua chlorido-complexes present in an HCl matrix. Under optimum chromatographic conditions it was possible, to separate and quantify cationic Rh(III) species (eluted as one band), $[RhCl_3(H_2O)_3]$, *cis*-$[RhCl_4(H_2O)_2]^-$, *trans*-$[RhCl_4(H_2O)_2]^-$ and $[RhCl_n(H_2O)_{6-n}]^{3-n}$ (n = 5, 6). The $[RhCl_n(H_2O)_{6-n}]^{3-n}$ (n = 5, 6) complex anions eluted as one band due to the relatively fast aquation of $[RhCl_6]^{3-}$ ($t_{1/2}$ = 1.3 min) in a low ionic strength (0.1 mol kg^{-1}) chloride matrix. It was found that the $t_{1/2}$ for $[RhCl_6]^{3-}$ aquation decreased significantly from 6.5 to 1.3 min when decreasing the ionic strength from 4.0 to 0.1 mol kg^{-1} $HClO_4$. In this context ionic strength or the activity of water is a key parameter that determines whether $[RhCl_n(H_2O)_{6-n}]^{3-n}$ (n = 5, 6) complex anions can be chromatographically separated. An advantage of the developed ion-pair HPLC

speciation method compared to previous CE speciation studies [9–11] is that it is possible to separate, quantify and identify the *cis*- and *trans*-$[RhCl_4(H_2O)_2]^-$ stereoisomers.

The Rh(III) samples that was equilibrated in differing HCl concentrations for 2.8 years at 298 K was analyzed with the ion-pair HPLC method. This analysis yielded a partial Rh(III) aqua chlorido-complex species distribution diagram as a function of HCl concentration. This diagram for the first time show the distribution of the *cis*- and *trans*-$[RhCl_4(H_2O)_2]^-$ stereoisomers. Furthermore, it was found that relatively large amounts of 'highly' aquated $[RhCl_n(H_2O)_{6-n}]^{3-n}$ (n = 0–4) species persist in up to 3.0 mol L^{-1} HCl and in 1.0 mol L^{-1} HCl the abundance of the $[RhCl_5(H_2O)]^{2-}$ species is only 8–10% far from the 70–80% proposed previously [3]. Interestingly a 95% abundance of the $[RhCl_6]^{3-}$ complex anion occurs only when the HCl concentration is above 6 mol L^{-1}. Work on extending the analysis of Rh(III) aqua halido-complexes speciation and to the other PGM are currently under way.

Acknowledgements

We gratefully acknowledge the financial support by Anglo-platinum Ltd., Nelson Mandela Metropolitan and Stellenbosch Universities.

Appendix A. Supplementary data

Supplementary data associated with this article can be found, in the online version, at doi:10.1016/j.talanta.2010.04.049.

References

[1] G. Schmukler, B. Limoni-Relis, Sep. Sci. Technol. 30 (3) (1995) 337.
[2] F.L. Bernardis, R.A. Grant, D.C. Sherrington, React. Funct. Polym. 65 (2005) 205.
[3] E. Benguerel, G.P. Demopoulos, G.B. Harris, Hydrometallurgy 40 (1996) 135.
[4] M.C. Read, J. Glaser, M. Sandström, J. Chem. Soc., Dalton Trans. 2 (1992) 233.
[5] C. Carr, J. Glaser, M. Sandström, Inorg. Chim. Acta 131 (1987) 153.
[6] B.E. Mann, C.M. Spencer, Inorg. Chim. Acta 76 (1983) L65.
[7] J.M. Ernsting, S. Gaemers, C.J. Elsevier, Magn. Reson. Chem. 42 (2004) 721.
[8] S.S. Aleksenko, A.P. Gumenyuk, S.P. Mushtakova, L.F. Kozhina, A.R. Timerbaev, Talanta 61 (2003) 195.
[9] S.S. Aleksenko, A.P. Gumenyuk, S.P. Mushtakova, J. Anal. Chem. 57 (2002) 215.
[10] S.S. Aleksenko, A.P. Gumenyuk, S.P. Mushtakova, A.R. Timerbaev, Fresenius J. Anal. Chem. 370 (2001) 865.
[11] J.M. Sánchez, M. Hidalgo, J. Havel, V. Salvadó, Talanta 56 (2002) 1061.
[12] D.A. Palmer, G.M. Harris, Inorg. Chem. 14 (1975) 1316.
[13] W.C. Wolsey, C.A. Reynolds, J. Kleinberg, Inorg. Chem. 2 (1963) 463.
[14] J. Kramer, K.R. Koch, Inorg. Chem. 45 (2006) 7843.
[15] J. Kramer, K.R. Koch, Inorg. Chem. 46 (2007) 7466.
[16] W.J. Gerber, P. Murray, K.R. Koch, Dalton Trans. 31 (2008) 4113.
[17] W. Robb, G.M. Harris, J. Am. Chem. Soc. 87 (1965) 4472.
[18] W. Robb, M.M. de V. Steyn, Inorg. Chem. 6 (1966 or 1967) 616.
[19] W. Robb, M.M. de, V. Steyn, H. Kruger, Inorg. Chim. Acta 3 (1969) 383.
[20] S.F. Chan, G.M. Harris, Inorg. Chem. 18 (1979) 717.
[21] R.J. Buchacek, G.M. Harris, Inorg. Chem. 15 (1976) 926.
[22] M.J. Pavelich, G.M. Harris, Inorg. Chem. 12 (1973) 423.
[23] K. Swaminathan, G.M. Harris, J. Am. Chem. Soc. 88 (1966) 4411.
[24] J.M. Sánchez, V. Salvadó, J. Havel, J. Chromatogr. A 834 (1999) 329.
[25] J.J. Kirkland, J.J. DeStefano, J. Chromatogr. A 1126 (2006) 50.
[26] R.K. Gilpin, M.E. Gangoda, A.E. Krishen, J. Chromatogr. Sci. 20 (1982) 345.
[27] R.J. Silby, R.A. Alberty, M.G. Bawendi, Physical Chemistry, 4th ed., John Wiley & Sons, Inc., New York, USA, 2005.
[28] W.J. Gerber, Ph.D. Dissertation, University of Port Elizabeth, South Africa, 2005.
[29] R.L. Burden, J.D. Faires, Numerical Analysis, 6th ed., Brooks/Cole Publishing Company, 1997.
[30] J.A. Nelder, R. Mead, Comput. J. 7 (1965) 308.
[31] J. Polster, H. Dithmar, Phys. Chem. Chem. Phys. 3 (2001) 993.
[32] J. Polster, Chem. Phys. 240 (1999) 331.
[33] T.E. Geswindt, M.Sc. Dissertation, Nelson Mandela Metropolitan University, South Africa, 2009.
[34] D.V. McCalley, Anal. Chem. 78 (2006) 2532.
[35] W. Preetz, G. Peters, D. Bublitz, Chem. Rev. 96 (1996) 977.
[36] G. Levitin, G. Schmuckler, React. Funct. Polym. 54 (2003) 149.
[37] D. Cozzi, F. Pantani, J. Inorg. Nucl. Chem. 8 (1958) 385.